JOSA COMMUNICATIONS

Communications are short papers. Appropriate material for this section includes reports of incidental research results, comments on papers previously published, and short descriptions of theoretical and experimental techniques. Communications are handled much the same as regular papers. Proofs are provided.

Patterns in the ripple structure of Mie scattering

Christopher M. Sorensen and Dan Shi

Department of Physics, Kansas State University, Manhattan, Kansas 66506-2601

Received January 31, 2001; revised manuscript received May 8, 2001; accepted June 28, 2001

We study the ripple structure in the scattered intensity predicted by Mie scattering theory in the angular behavior of the scattered intensity for homogeneous, dielectric spheres. We find that for small values of the phase shift parameter $\rho = 2kR|m - 1|$, where $k = 2\pi/\lambda$, R is the sphere radius, and m is the relative refractive index, the ripples are periodic with spacing equal to π when plotted versus the dimensionless qR, where $q = 2k \sin(\theta/2)$ and θ is the scattering angle. However, as ρ increases, this outcome switches to nonuniform spacing of approximately $\pi \cos(\theta/2)$. The latter spacing is equivalent to a uniform spacing of π/kR when plotted versus θ.

OCIS codes: 290.4020, 290.5850.

1. INTRODUCTION

Scattering of light by uniform spheres is a central phenomenon in both natural and technical settings and is the basis for scattering from more complex systems. The problem of how light, an electromagnetic wave, scatters from a sphere was solved by Mie by 1908.[1] The solution is complex, both in the form of its equations and when displayed graphically. Because of this, many approximations or limiting situations of the Mie equations have been studied to gain some degree of simplicity and perhaps thereby physical insight.[2–4]

In this spirit we recently showed[5] that discernable patterns appear in the Mie result if the scattered intensity is plotted, not versus the scattering angle θ, the usual way, but versus the scattering wave vector

$$q = 4\pi\lambda^{-1} \sin(\theta/2) \tag{1}$$

where λ is the wavelength. In fact, an even better parameter is the dimensionless qR, where R is the sphere radius. Only scattering for the common experimental situation of incident light polarized normal to the scattering plane and scattered (detected) polarization unpolarized was considered, to avoid angle functionality that is due to polarization. The scattering may be viewed as composed of a series of maxima and minima, the ripples; the envelopes of these ripples; and the enhanced back scattering, or glory. The envelopes describe the overall, gross features of the scattering. The patterns appear in the envelopes of the curves of the scattered intensity I versus qR, i.e., if the interference ripple structure of the curves is ignored. Moreover, the patterns are functions of the phase shift parameter

$$\rho = 2kR|m - 1|, \tag{2}$$

where $k = 2\pi/\lambda$ and m is the sphere's index of refraction relative to the medium. This functionality is quasi-universal in that k, R, and m may vary but the same ρ leads to nearly the same curve. Our results are illustrated schematically in Fig. 1. For small ρ, I versus qR on a log–log plot shows no slope when $qR < 1$ but a slope of -4 for $qR > 1$. This is consistent with the Rayleigh–Debye–Gans (RDG) result and Porod scattering.[6] As ρ increases, the envelope of the Mie curve rises from the $\rho = 0$ limit, retaining the -4 slope for large qR but developing a -2 slope at intermediate qR. This trend continues with increasing ρ, with the rising curve bounded above by $I \simeq 2(qR)^{-2}$. In summary, if one ignores the ripples and the glory, Mie scattering displays three power-law regimes (the regime's boundaries are approximate):

$$I \propto (qR)^0 \qquad \text{when } qR < 1 \tag{3a}$$

$$I \propto (qR)^{-2} \qquad \text{when } 1 < qR < \rho \tag{3b}$$

$$I \propto (qR)^{-4} \qquad \text{when } qR > \rho. \tag{3c}$$

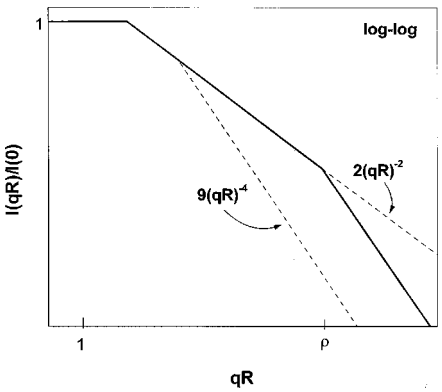

Fig. 1. Schematic diagram of the envelopes of the Mie scattering curves for homogeneous, dielectric spheres (i.e., ignoring the ripple structure). Dashed lines, RDG limit at $\rho = 0$ with slope -4 and the $\rho \to \infty$ limit with slope -2; solid line, envelope for an arbitrary ρ.

One obvious question arises: What about the ripples? In this short Communication we show that the ripples in the Mie scattering show a simple pattern that does not appear to have been described before.

2. RESULTS

We start in the limit of $\rho = 0$, where the Mie equations reduce to the RDG result

$$I(u) = [3(\sin u - u \cos u)/u^3]^2, \tag{4}$$

where $u = qR$. It is straightforward to show that the periodicity of this function is π. We will say that the spacing (in qR space) between the ripples is π and express this as $\delta_{qR} = \pi$. How does the spacing δ_{qR} behave as ρ increases above zero and the Mie scattering becomes more complex?

To answer this question we look at the Mie results empirically in graphical form rather than examining the algebraic structure of the equations. The program BHMIE from Bohren and Huffman[4] was used to generate plots of I versus qR for a wide variety of size parameters, kR, and refractive indices, m. Only scattering for the common experimental situation of incident polarization vertical, no polarizer on the detector (with θ in the horizontal plane) was considered to avoid functionality due to polarization.

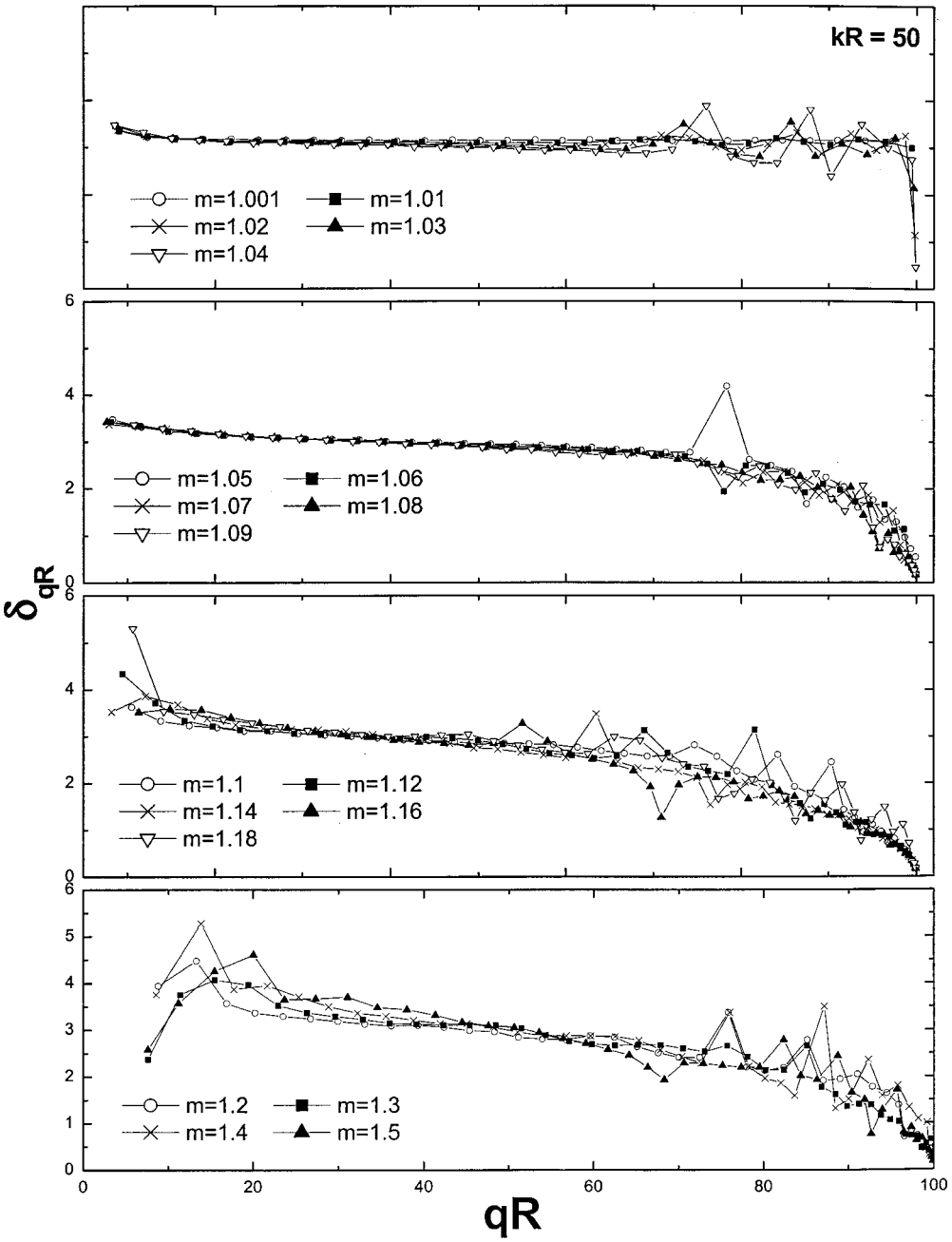

Fig. 2. Spacing between successive maxima for the scattered light intensity for spheres with a size parameter of $kR = 50$ but different indices of refractions m, hence different phase shift parameters ρ.

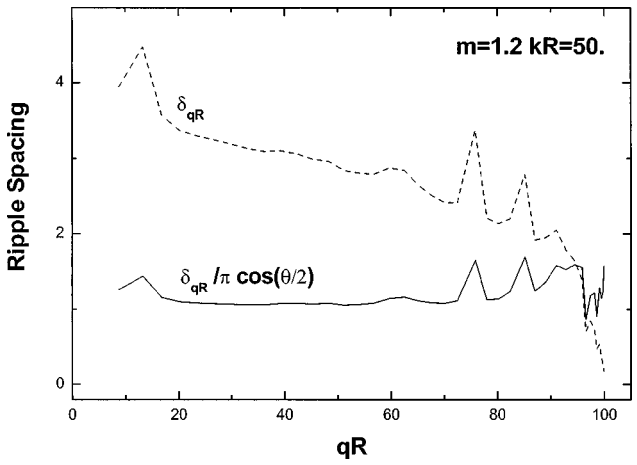

Fig. 3. Ripple spacing plotted as either δ_{qR} or $\delta_{qR}/\pi\cos(\theta/2)$.

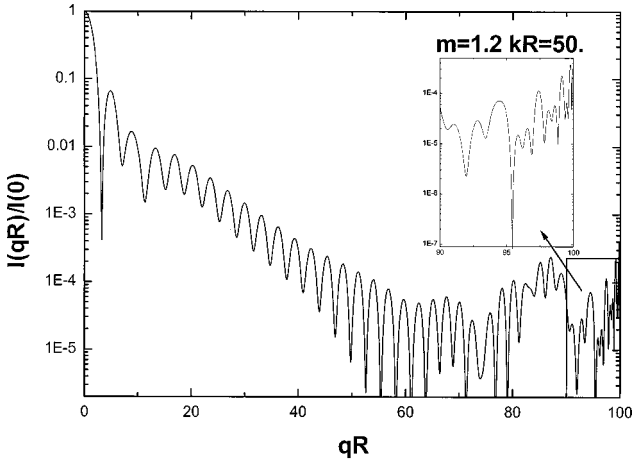

Fig. 4. Normalized Mie scattered intensity for spheres with $m = 1.2$ and $kR = 50$, hence $\rho = 20$ versus qR. Note how the ripple spacing becomes smaller at large qR.

A program was written to find sequential, local maxima in the plots and from these determine their spacing δ_{qR} as a function of qR.

Typical results are shown in Fig. 2 for a size parameter of $kR = 50$. For small m ($m \leq 1.04$) the spacing is still approximately equal to π with some minor fluctuations. This is a consistent extension of the $\rho = 0$, Eq. (4), RDG result. As m increases, some deviation to values greater than π appear at small qR. By the time $m \geq 1.05$, which corresponds to $\rho \geq 5$ for $kR = 50$, a new trend sets in that can be described by a $\cos(\theta/2)$ functionality. This is illustrated in Fig. 3, where the spacing δ_{qR} is plotted, as well as $\delta_{qR}/\pi\cos(\theta/2)$. The latter is fairly constant, ignoring the noise, for the entire range of qR. Finally, for yet larger values of m ($m > 1.10$) and ρ, Fig. 2 shows that some more noise sets in around the $\pi\cos(\theta/2)$ functionality, and the deviation to values greater than π increases at small qR. Similar results are found for other size parameters. We summarize the ripple spacing for spherical particle Mie scattering as

$$\delta_{qR} = \pi, \qquad \rho < 1, \tag{5a}$$

$$\delta_{qR} = \pi\cos(\theta/2), \qquad \rho \geq 5. \tag{5b}$$

The noise in these results is real; i.e., although the trends are described by Eqs. (5), there can be deviations from Eqs. (5) for the spacings between individual, adjacent pairs of peaks. No pattern could be discerned for this behavior, which was persistent for all ρ.

The ripple spacing for large ρ in Eq. (5b) implies uniform spacing if the intensity is plotted versus θ. This is easily shown by multiplying q of Eq. (1) by R, and differentiating to find

$$\frac{d(qR)}{d\theta} = kR\cos(\theta/2). \tag{6}$$

This combined with Eq. (5b) implies for large ρ that the ripple spacing in θ-space is

$$\delta\theta = \pi/kR, \qquad \rho \geq 5. \tag{7}$$

Examples of these ripple structures are given in Figs. 4 and 5 for $kR = 50$ and $m = 1.2$; hence $\rho = 20$. In Fig. 4 the scattered intensity is plotted versus qR, and one can see that the spacing between ripples is $\sim\pi$ for small qR but decreases almost to zero as qR increases to its maximum value of $2kR$. The same scattering is plotted versus θ in Fig. 5, and there one readily sees the uniformity

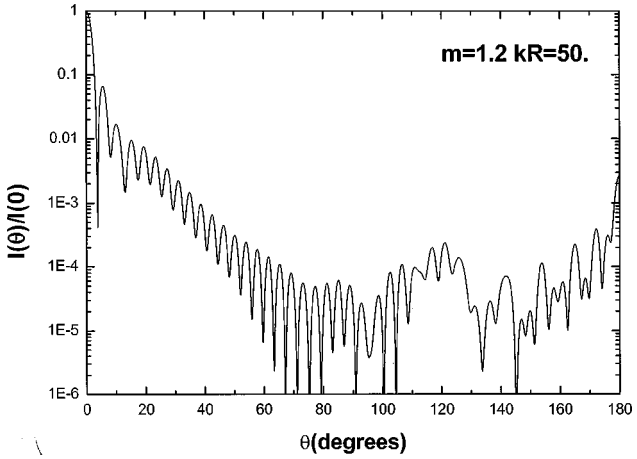

Fig. 5. Normalized Mie scattered intensity for spheres with $m = 1.2$ and $kR = 50$, hence $\rho = 20$ versus θ. Note how the ripple spacing remains constant at large θ.

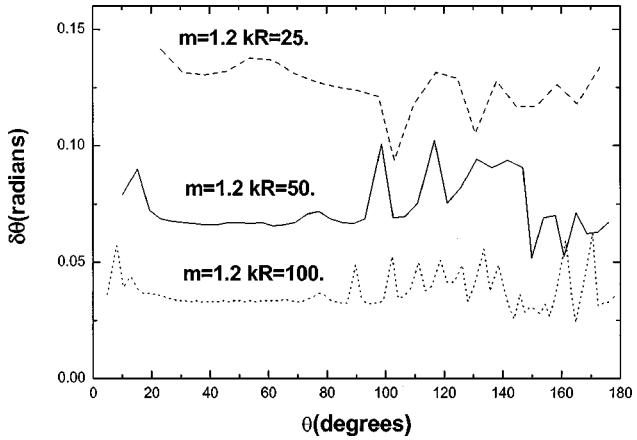

Fig. 6. Ripple spacing in θ space, $\delta\theta$, as a function of scattering angle.

of the ripple spacing when it is plotted versus θ. Figure 6 demonstrates Eq. (7) for three different size parameters.

Nearly 40 years ago Maron *et al.*[7,8] and Kerker *et al.*[9] studied the spacing in the ripple structure of spherical particle Mie scattering. Their results were expressed as

$$2R\lambda^{-1}\sin(\theta/2) = k_i \quad \text{or} \quad K_i. \tag{8}$$

In Eq. (8) k_i are positions of the minima; K_i are positions of the maxima. Multiplied by 2π, the left-hand side of Eq. (8) becomes qR. The ripple spacing is thus $\delta_{qR} = 2\pi\delta K_i$ (we consider only maxima). Their tabulated values of K_i are consistent with our conclusions, but the pattern of a crossover from the behavior of Eq. (5a) to the behavior of Eq. (5b) is not described in this previous work because it did not consider large-angle behavior. The vast improvement in computing power has allowed us to see this pattern. The purpose of this previous work was particle sizing for monodisperse systems (modest polydispersity, however, washes out the ripples, leaving only the envelopes). This possibility remains in light of our work through either Eq. (5) or (7).

3. DISCUSSION AND CONCLUSION

A physical explanation for this crossover in spacing of the ripples from uniform in qR space to uniform in θ space with increasing ρ remains a mystery to us. In our previous work[5] we explained the curve envelope patterns in Eqs. (3) as due to the localization of the scattering to a shell just within the surface of the sphere. This shell's thickness is inversely proportional to ρ. This model, however, predicts the ripple spacing to remain uniform in qR space with the value of π regardless of ρ. Hence the physics that guides the envelopes of the curves does not appear to affect the behavior of the ripples underneath the envelopes. Finally, we should not fail to point out that Eq. (7) is equivalent to $\delta\theta = \lambda/D$, where D is the particle diameter. This is the canonical Fraunhofer result for fringe spacing due to coherent point sources separated by D. How this applies to the extended sphere is yet another mystery.

ACKNOWLEDGMENT

This work was supported by National Science Foundation grants CTS9709764 and CTS0080017.

C. Sorensen can be reached at the address on the title page or by e-mail, sor@phys.ksu.edu.

REFERENCES

1. G. Mie, "Beitrage zur Optik trüber Medien speziel kolloidaler Metallösungen," Ann. Phys. **25**, 377–445 (1908).
2. H. C. van de Hulst, *Light Scattering by Small Particles* (Dover, New York, 1981).
3. M. Kerker, *The Scattering of Light and other Electromagnetic Radiation* (Academic, New York, 1969).
4. C. F. Bohren and D. R. Huffman, *Absorption and Scattering of Light by Small Particles* (Wiley, New York, 1983).
5. C. M. Sorensen and D. J. Fischbach, "Patterns in Mie scattering," Opt. Commun. **173**, 145–153 (2000).
6. A. Guinier, G. Gournet, C. B. Walker, and K. L. Yudowitch, *Small Angle Scattering of X-Rays* (Wiley, New York, 1955).
7. S. H. Maron and M. E. Elder, "Determination of latex particle size by light scattering I. Minimum intensity method," J. Colloid Sci. **18**, 107–118 (1963).
8. P. E. Pierce and S. H. Maron, "Prediction of minima and maxima in intensities of scattered light and of higher order Tyndall spectra," J. Colloid Sci. **19**, 658–672 (1964).
9. M. Kerker, W. A. Farone, L. B. Smith, and E. Matijevic, "Determination of particle size by the minima and maxima in the angular dependence of the scattered light. Range of validity of the method," J. Colloid Sci. **19**, 193–200 (1964).